

## Substrate Temperature effect on the Physical properties of Spray deposited Lead sulfide Thin Films suitable for Solar control coatings

C.Rajashree<sup>1</sup>, A.R. Balu<sup>1\*</sup>, V.S.Nagarethinam<sup>1</sup>

<sup>1</sup>AVVM Sri Pushpam College, Poondi – 613 503, Thanjavur Dt, Tamilnadu, India

\*Corres.author: rajavelubalu@yahoo.com  
Ph: +91 9442846351

**Abstract:** Lead sulfide thin films were deposited at three different substrate temperatures on glass substrates by cost effective spray pyrolysis technique using lead acetate as cationic precursor and thiourea as anionic precursor. The X-ray diffraction study showed that irrespective of substrate temperature all the films exhibits a preferred orientation along the (1 1 1) plane. The values of crystallite size were found to be in the range 38 – 65 nm. The percentage transmittance increases from 67 % to 77 % with increase in substrate temperature. Optical band gap value decreases from 1.96 eV to 1.87 eV with increase in substrate temperature. Urbach energy decreases with increase in substrate temperature. The values of refractive index and packing density for the film coated at 300°C were found to be equal to 2.35 and 4.29 respectively. A minimum electrical resistivity of  $0.085 \times 10^5$  ohm-cm was obtained for the film coated at 300°C. The dispersion parameters of the as deposited films were calculated to analyze their choice in designing optical devices.

**Keywords:** Thin films; X-ray diffraction; Surface morphology; Optical studies; Band gap energy; Electrical properties.

### 1. Introduction

Semiconducting materials have outstanding electronic and optical properties which make them suitable for potential application in various devices such as light emitting diodes [1], single electron transistors [2] and field effect thin films transistors [3]. Most studied semiconductors belong to the II-VI and IV-VI groups, since they are relatively easy to synthesize and are generally prepared as particles or in thin film form in the recent years [4]. Lead sulfide (PbS) belongs to the IV-VI group –  $A_4B_6$  semiconductor with a narrow band gap of 0.41 eV at room temperature and 0.29 eV at liquid –  $N_2$  temperature. Thin films of PbS have been a subject of interest for many years, mainly because of their photoconductive properties, in the 1000 – 3000 nm spectral range at room temperature, and is used for manufacturing photoconductive cells that are of interest in a variety of applications both in domestic life and military domains. Being a narrow gap semiconductor, PbS has a bulk band gap in the near IR [5]. Its emission and absorption lines are consequently broader, but by monitoring its crystallite size, tunable emission can be obtained in a large spectral region, ranging from the visible to near infrared. This spectral range is of great interest for fabricating light sources (including lasers) or optical

amplifiers. PbS films deposited on glass substrates possess excellent solar control characteristics comparable to the metallic films [6 – 9]. Lead sulfide films has attracted considerable attention owing to a larger excitation Bohr radius of 18 nm [10] and has been widely used in many fields such as Pb<sup>2+</sup> ion-selective sensors [11], photography [12], IR detectors [13], and solar absorbers [14]. In solar energy research, PbS thin films were investigated for photothermal conversion applications, either independently on metallic substrates or in multi-layer stacks of PbS-CdS-PbS, (PbS)<sub>1-x</sub>(CdS)<sub>x</sub> composites. Solar control applications of PbS thin films of 0.05 – 0.15 μm thickness were deposited on glass substrates in single layers [6, 8]. PbS thin films can be fabricated by various deposition techniques such as electro deposition [15], spray pyrolysis [16], photo accelerated chemical deposition [17], microwave heating [18, 19] and chemical bath deposition CBD [20 – 24]. Of all these techniques, spray pyrolysis appears as an interesting technique for preparing thin films [25, 26]. The spray technique of preparation of thin films is very attractive because it is inexpensive, simple and capable of deposition of optically, smooth, uniform and homogeneous layers. Film growth can be easily controlled by preparative parameters such as spray rate, substrate temperature, concentration of solution, nozzle frequency, etc [27, 28]. In this work, spray pyrolysis technique is employed to coat PbS thin films and one of the spray parameter viz. substrate temperature is varied as 200, 250 and 300°C. The influence of substrate temperature on the structural, morphological, optical and electrical properties of the coated samples was observed and the results are reported.

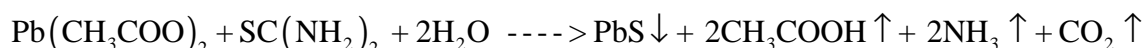
## 2. Experimental Details

Thin films of lead sulfide were prepared by spraying an aqueous solution containing 0.025 M of lead acetate and 0.025 M of thiourea (S/Pb molar ratio = 1) on glass substrates (dimensions – 76 mm x 25 mm x 1.4 mm) kept at 200, 250 and 300°C. The atomization of the chemical solution into a spray of fine droplets is effected by the spray nozzle, with the help of compressed air as carrier gas. The film thickness was measured by means of weight gain method and compared with the values determined by employing a profilometer (Surftest SJ 301). The structural analysis was made using X-ray diffractometer (PANalytical – PW 340 / 60 X'pert PRO) with CuKα radiation of wavelength 1.5406 Å operated at 40 kV and 30 mA in the 2θ range 10° to 80°. SEM images were obtained using Scanning Electron Microscope (HITACHI S-3000H). The optical transmission spectra were recorded in the 300 – 1100 nm wavelength region by using a Perkin Elmer UV-Vis-NIR double beam spectrophotometer (LAMDA – 35). The electrical resistivity (ρ), was determined using d.c. two point probe technique at room temperature.

## 3 Results And Discussion

### 3.1 Film Formation Process

The precursor solution was atomized to form uniform stream of fine droplets with pneumatic glass nozzle. The pyrolytic decomposition of the fine droplets of aqueous solution of lead acetate and thiourea onto the glass substrates results into the formation of thin films of PbS which were slightly black grayish in colour. The possible chemical reaction that takes place is as follows:



The thicknesses of the films coated at substrate temperatures of 200, 250 and 300°C were found to be equal to 0.72 μm, 0.67 μm and 0.63 μm respectively. It is observed that as the substrate temperature increases, the film thickness decreases despite the fact that the kinetics of the film forming reaction should increase with growth temperature. This can be explained by the diminished mass transport to the substrate at higher temperature or it can be attributed to an increase in the rate of re-evaporation at higher temperatures. Similar results were reported by Afifi *et. al* [29]. The low value of thickness obtained for the PbS film coated at 300°C strongly favors the reduction of grain boundary scattering which results in the improvement of its crystallinity as evident from the XRD analysis (section 3.2). The improvement in crystallinity signifies that the dislocations and density of grain boundaries decrease leading to a decrease of donor sites trapped at the dislocations and grain boundaries [30].

### 3.2 Structural Studies

The X-ray diffraction profile of the PbS thin films is represented in Fig. 1.

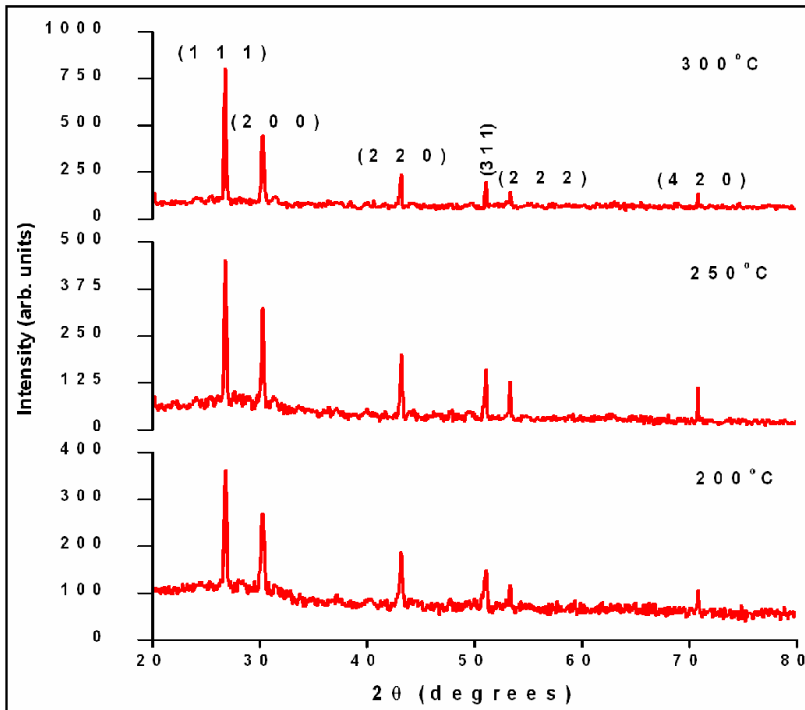


Fig. 1

XRD patterns of PbS films deposited at different substrate temperatures.

All the PbS films are polycrystalline in nature with face centered cubic structure as confirmed by JCPDS No. 5-0592 for galena PbS. XRD patterns of all the PbS thin films showed sharp (1 1 1) and (2 0 0) peaks along with minor peaks of (2 2 0), (3 1 1), (2 2 2) and (4 2 0) planes corresponding the face centered cubic structure of PbS. The preferential orientation factor  $f(h\ k\ l)$  of the prominent peaks ((1 1 1), (2 0 0), (2 2 0), (3 1 1) and (2 2 2)) of the sprayed PbS films were calculated and given in Table 1. For all the films the preferential orientation value of (1 1 1) plane has the highest value compared to that of the other planes indicating a strong orientational growth along that plane. This result on preferential orientation is strongly supported with earlier report [31]. The variation in preferential orientation factor  $f(h\ k\ l)$  for (1 1 1) as a function of substrate temperature shown in Fig. 2, predicts that  $f(1\ 1\ 1)$  is maximum for the film coated at 300°C, indicating better crystallinity.

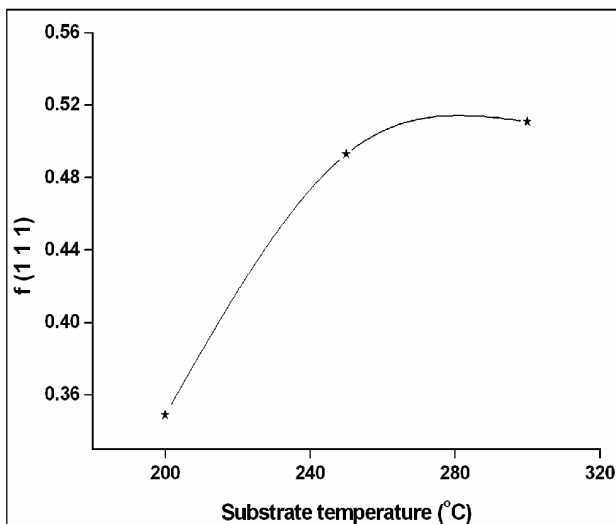


Fig. 2

Variation of preferential orientation factor  $f(1\ 1\ 1)$  of PbS films with substrate temperature.

The intensity of the peaks increases with increase in substrate temperature which reveals that crystallinity of the film improves with increase in substrate temperature. The reduction of micro strain values at higher temperature (Table 3) might be the reason for the improved crystallinity of PbS film coated at 300°C.

The observed d- spacings of the (1 1 1), (2 0 0), (2 2 0) (3 1 1), (2 2 2) and (4 2 0) planes of the PbS films along with the standard d-spacing values (JCPDS standards Card No. 5-0592) are listed in Table 2. The interplanar distance for (1 1 1) plane of the PbS film coated at 300°C exactly matches with the standard value while the values of ‘d’ for the films coated at 200°C and 250°C appears to be smaller than the standard value. This indicates contraction of unit cell volume that in turn reveals that the samples coated at 200 and 250°C are strained.

The lattice constant ‘a’ is calculated using the formula:

$$\frac{1}{d^2} = \frac{h^2 + k^2 + l^2}{a^2} \tag{1}$$

The lattice parameter values calculated for the (1 1 1) plane are given in Table. 3. The lattice constant values are found to be lesser than the bulk sample (a = 5.936Å) confirming the strain present in the samples. The deviation of the lattice parameter values may be due to the presence of residuals of the reaction components especially carbon in the films. Various structural parameters, e.g. Crystallite size (D), dislocation density (δ) and strain (ε) calculated for the (1 1 1) plane are presented in Table. 3. The crystal defect parameters like microstrain and dislocation density show a decreasing trend with increase in substrate temperature. This type of change in strain may be due to the recrystallization process in the polycrystalline films. At higher temperature deposition, both the microstrain and dislocation density are minimum, which reveals the reduction in the concentration of lattice imperfections leading to preferred orientations [32]. As the dislocation density is the measure of the defects in the crystalline structure, the larger value of δ obtained for the film coated at 200°C showed that the film has comparatively lesser degree of crystallinity.

**Table 1: Preferential orientation factor of PbS thin films fabricated at different substrate temperatures**

Substrate temperature (°C)	f(h k l)				
	f(1 1 1)	f(2 0 0)	f(2 2 0)	f(3 1 1)	f(2 2 2)
200	0.301	0.2502	0.11	0.046	0.045
250	0.421	0.163	0.046	0.049	0.024
300	0.4635	0.1762	0.045	0.033	0.0302

**Table 2: Comparison of observed and standard ‘d’ values for the PbS films coated at three substrate temperatures.**

d (standard) Å	d (observed) Å			(h k l)
	200°C	250°C	300°C	
3.429	3.425	3.427	3.429	(1 1 1)
2.969	2.949	2.952	2.960	(2 0 0)
2.099	2.094	2.092	2.096	(2 2 0)
1.790	1.842	1.840	1.841	(3 1 1)
1.740	1.730	1.732	1.736	(2 2 2)
1.327	1.334	1.331	1.330	(4 2 0)

**Table 3: Calculated microstructural parameters associated with PbS thin films.**

Substrate temperature (°C)	Microstructural parameters			
	a (Å)	D (nm)	$\epsilon$ ( $\times 10^{-4}$ )	$\delta$ ( $\times 10^{14}$ lines/m <sup>2</sup> )
200	5.759	38.8	9.6	6.64
250	5.762	44.9	8.3	4.96
300	5.766	65.6	5.7	2.32

### 3.3 Surface morphological studies

The SEM images of the PbS films are shown in Fig. 3.

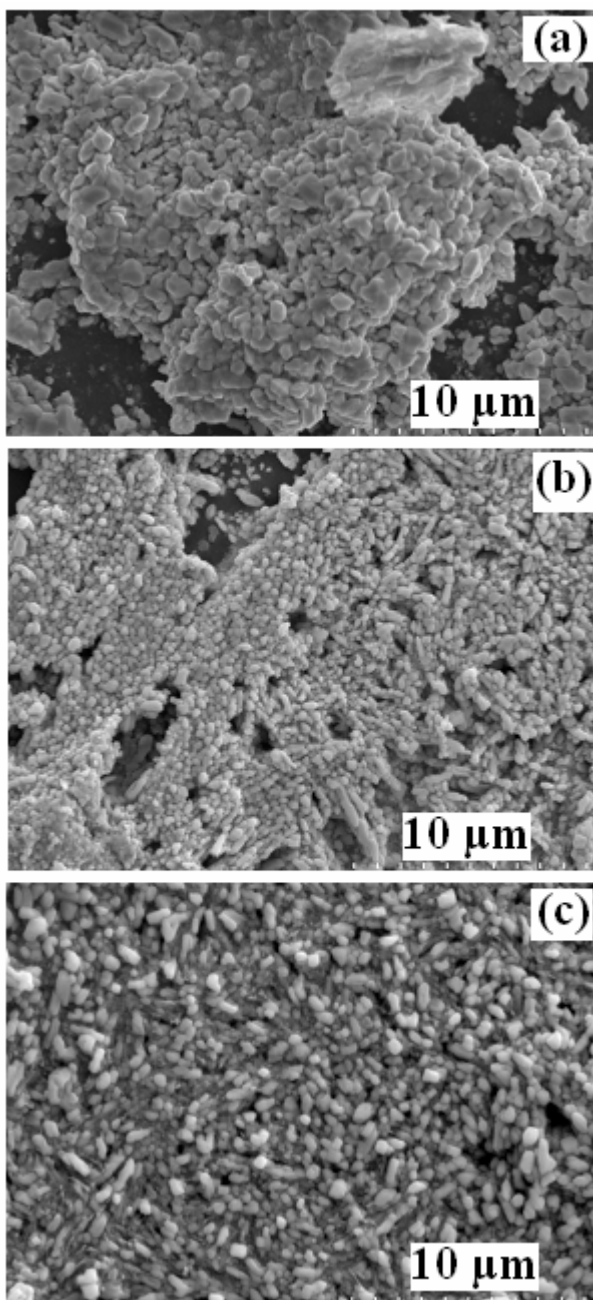


**Fig. 3**

SEM images of the as-deposited PbS films.

SEM image of the film coated at 200°C (Fig 3a) showed clusters of grains bounded together which might be due incomplete vaporization of the droplets before reaching the substrate surface. Grains appeared tightly packed for the PbS film coated at 250°C (Fig. 3b). Cluster formation is minimized indicating improvement in the vaporization of the droplets reaching the substrate surface. The SEM image of the film coated at 300°C (Fig. 3c) showed uniform surface with well-defined grain boundaries. No cluster formation is observed and the grains appear uniform suggesting that there was a uniform nucleation throughout the surface.

### 3.4 Optical studies

Study of materials by means of optical absorption provides a simple method for explaining some features concerning the band structure of materials. Optical absorption measurements of PbS films were carried out in the wavelength range 300 – 1100 nm. Fig. 4 shows the variation of absorbance with wavelength of the as-deposited PbS samples.

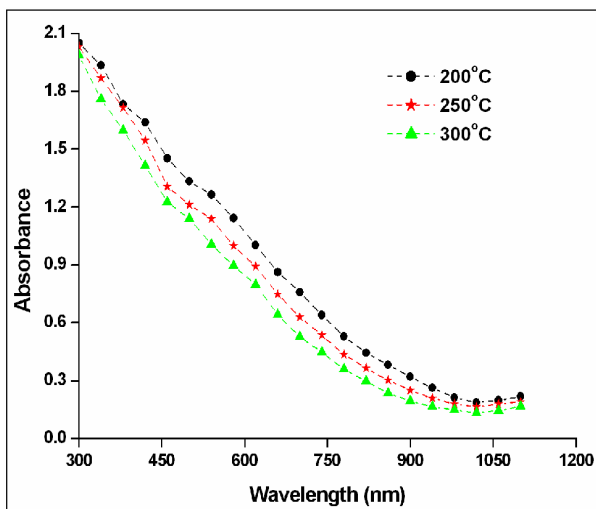


Fig. 4

#### Variation of Absorbance of PbS thin films with wavelength.

The spectra show two regions, one for higher wavelength (> 1000 nm) showing practically low absorption and other for lower wavelength (< 900 nm) in which absorption increases rapidly for all the samples. Similar results were obtained by Preetha et. al [31] for SILAR deposited PbS films.

The optical absorption coefficient ( $\alpha$ ) was calculated for each film from the absorption spectra using the relation:

$$\alpha = \frac{2.303A}{t} \quad (2)$$

where t is the thickness and A is the absorbance of the as-deposited PbS films. The absorption coefficient ( $\alpha$ ) is related to the band gap of the material by the equation [33]:

$$(\alpha h\nu) = A(h\nu - E_g)^n \quad (3)$$

where  $n = 1/2$  for allowed direct transition and  $n = 2$  for indirect transition, A is the parameter which depends of the transition probability. In Fig.5, the relationship between  $(\alpha h\nu)^2$  and  $h\nu$  is plotted. The energy band gap values can be obtained by extrapolating the linear portion to the photon energy axis.

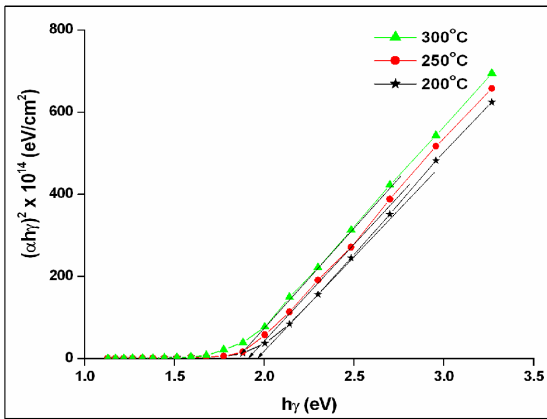


Fig. 5

Variation of  $(\alpha h\gamma)^2$  with photon energy ( $h\gamma$ ) of as-deposited PbS films.

The obtained  $E_g$  values are in good agreement with the earlier reported values [33].

Tauc [34] has identified three distinct regions in the absorption spectrum of amorphous semiconductors: a) the weak-absorption tail which originates from defects and impurities, b) the exponential edge region which is strongly related to the structural randomness of the glassy material, and c) the high absorption edge region which determines the optical energy gap. In the exponential edge region the absorption coefficient  $\alpha(h\gamma)$  is well described by the exponential law

$$\alpha = \alpha_0 \exp\left(\frac{h\gamma}{E_u}\right) \tag{4}$$

known as Urbach law [35]. Here  $\alpha_0$  is a constant,  $h\gamma$  is the incident photon energy, and  $E_u$  is called Urbach energy, which characterizes the slope of the exponential edge region and is width of the band tails of the localized states. The Urbach tail of the absorption edge is usually ascribed to the optical electronic transitions between the excited states and the near edge localized states. The formation of localized states with energies at the boundaries of the energy gap is one of the effects of the structural disorder on the electronic structure of amorphous materials. This is the reason why the Urbach energy is frequently used as a measure of the degree of structural disorder.  $E_u$  is given by the relation:

$$E_u = \left[ \frac{d(\ln(\alpha))}{d(h\gamma)} \right]^{-1} \tag{5}$$

The graph of  $\ln(\alpha)$  versus  $h\gamma$  being the photon energy is given in Fig. 6.

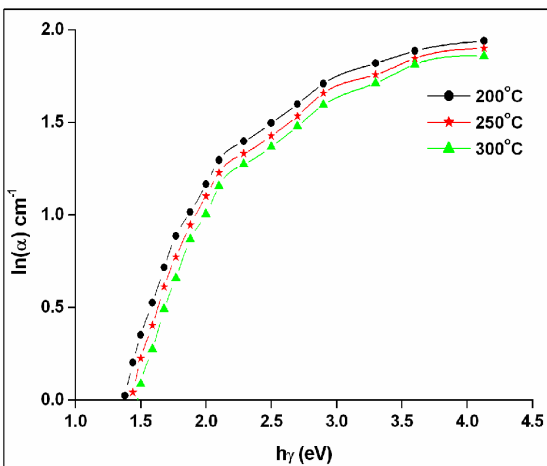


Fig. 6

Variation of  $\ln(\alpha)$  with photon energy ( $h\gamma$ ).

The value of  $E_u$  is calculated from the slope of the linear plot illustrated in Fig. 6. The variation of band gap energy ( $E_g$ ) and Urbach energy ( $E_u$ ) of PbS thin films with substrate temperature is shown in Fig. 7.

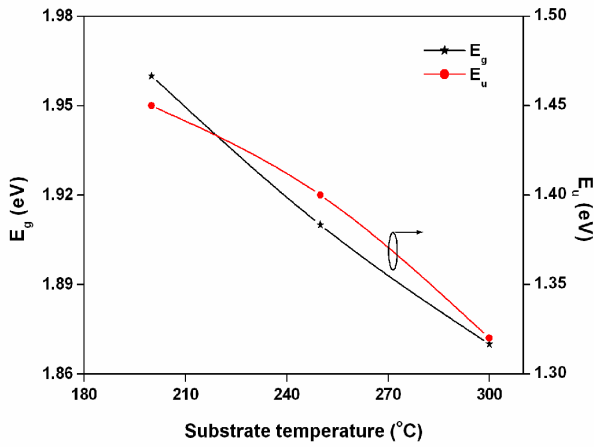


Fig. 7

**Variation of band gap energy and Urbach energy with substrate temperature of PbS films.**

As evident from Fig. 7, the  $E_g$  values of PbS films decreases with increase in substrate temperature which lies in the red region of the visible spectrum due to agglomeration of the nano-crystallites into larger crystallites [31]. The minimum value of  $E_u$  obtained at 300°C, indicates a very weak absorption tail due to minimized defects and impurities which improves the transparency and optical conductivity of the film coated at that temperature.

Fig. 8 shows the transmittance and reflectance spectra of the as-deposited PbS films.

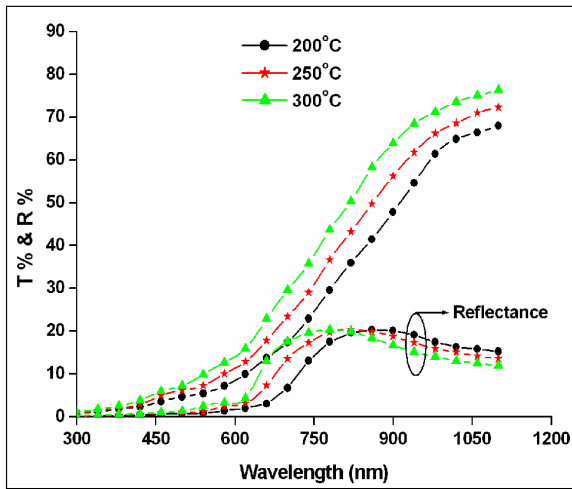


Fig. 8

**Transmittance and Reflectance spectra of PbS thin films.**

The percentage transmittance increases with increase in substrate temperature and the film coated at 300°C has a maximum transmittance of nearly equal to 77 %. The high percentage transmittance value for the PbS film coated at 300°C may be attributed to the uniform, well adherent and highly crystalline nature of the film as revealed from the XRD results that showed high peak intensities due to uniform nucleation and improvement in lattice arrangements [36]. Also it can be seen that the values of percentage transmittance of all PbS films takes a very low value in the wavelength region ( $\lambda < 500$  nm) which is the spectral region of edge absorption where the incoming photons have sufficient energy to excite electrons from the valence band to the conduction band and thus these photons are absorbed within the material to decrease the transmittance. All the samples can be used as solar control coatings as they have very low optical transmittance in the UV and in the visible region upto 600 nm and an appreciable reflection in the NIR region [37]. High reflection in the NIR region ensures that the obtained PbS films can minimize the temperature inside buildings.

Refractive index is one of the fundamental properties for an optical material because it is closely related to the electronic polarization of ions and the local field inside materials. The complex optical constant (refractive index, (n)) of the as-deposited PbS films has been evaluated by the relation [38]:

$$n = \frac{1+R}{1-R} \pm \sqrt{\frac{4R}{(1-R)^2} - k^2} \tag{6}$$

where  $k = \frac{\alpha\lambda}{4\pi}$  is the extinction coefficient. The obtained values of refractive index, extinction coefficient of the PbS films are presented in Table 4.

**Table 4: Optical parameters of PbS films fabricated by spray pyrolysis technique at different substrate temperatures**

Substrate temperature (°C)	Refractive index (n)	Extinction coefficient (k x 10 <sup>-3</sup> )	Packing density (p)
200	2.8	62	3.65
250	2.64	51	4
300	2.35	43	4.29

The high value of ‘n’ obtained for the PbS film coated at 200°C can be attributed to an increase of its surface roughness which acts to decrease the effective mean free path through increased surface scattering [39] and this fact strongly favors the reason for the reduction of its transparency. This fact is again supported by the high value of ‘k’ obtained for the film coated at 200°C which indicates high absorption and reduced transmittance as the variation in extinction coefficient is paralleled by the absorbance of the PbS films.

Fig. 9 shows the plot of refractive index in the NIR as a function of wavelength (λ) for PbS films fabricated at different substrate temperatures. The refractive index of the films decreases with the increase of λ and the rate of variation ceases at the higher wavelength region, i.e.  $\frac{dn}{d\lambda} < 0$ . The lower values of ‘n’ in the NIR is an indication that the rate at which light is slowed down in the film decays sharply to relatively low rate in the NIR which is similar to the behavior reported earlier [40]. The dispersion relation for refractive index fits well and explains the variation obtained for PbS films. The dispersion energy E<sub>d</sub> and the single oscillator energy E<sub>o</sub> are obtained in terms of the single oscillator model and these values are related to the refractive index as

$$n^2 - 1 = \frac{E_d E_o}{E_o^2 - (h\gamma)^2} \tag{7}$$

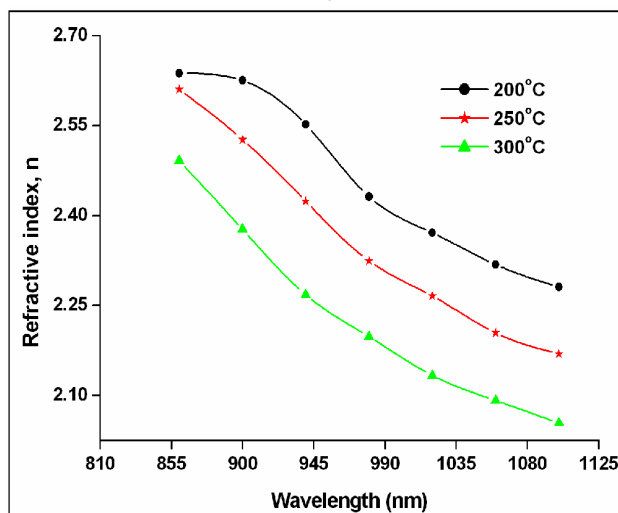


Fig. 9

Plot of NIR refractive index (n) of PbS films fabricated at different substrate temperatures.

The values of  $E_o$  and  $E_d$  for interband optical transitions are calculated and found to be 3.8 and 7.34 eV respectively. From these values, the long wavelength limit of refractive index  $n_\infty$  can be determined using the expression:

$$n_\infty = \sqrt{1 + E_d / E_o} \quad (8)$$

The long wavelength ( $1/\lambda \approx 0$ ) limit refractive index of the PbS films was calculated and the observed value of  $n_\infty = 2.93$  is consistent with the reported values [41].

From the refractive index data, the packing density ( $p$ ) which is defined as the ratio of the solid volume to the total volume of the film is estimated using the relation [42]:

$$n^2 = \frac{(1-p)n_v^4 + (1+p)n_v n_s^2}{(1+p)n_v^2 + (1-p)n_s^2} \quad (9)$$

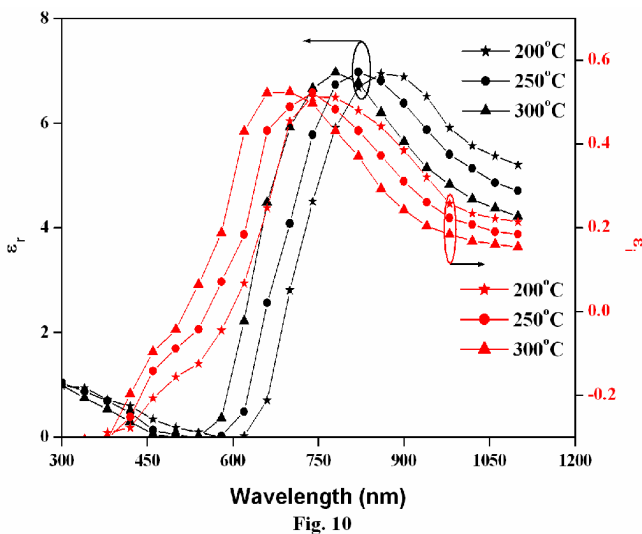
where  $n$  is the refractive index of the as-deposited PbS films,  $n_s$  is the refractive index of the bulk PbS material and  $n_v$  is the refractive index of voids, which are generally filled with ambient, i.e. air. The calculated values of packing density are presented in Table 4. The packing density increases with substrate temperature indicating the improvement of crystallinity of the PbS films as substrate temperature increases.

It is well known that polarizability of any solid is proportional to its dielectric constant. The real and imaginary parts of the complex dielectric constant are expressed as [43]:

$$\epsilon_r = n^2 - k^2 \quad (10)$$

$$\epsilon_i = 2nk \quad (11)$$

where  $\epsilon_r$  and  $\epsilon_i$  are the real and imaginary parts of the dielectric constants, respectively. The variation of  $\epsilon_r$  and  $\epsilon_i$  with wavelength of the as-deposited PbS films are shown in Fig. 10.



**Wavelength dependence of the real and imaginary parts of dielectric constants.**

The real and imaginary parts of dielectric constants follow the same trend. The variation of the dielectric constants with photon energy indicates that some interactions between photons and electrons in the films are produced in this energy range. The imaginary part of dielectric constant is directly related to the density of states within the forbidden gap of semiconductor materials [44].

### 3.5 Electrical studies

The resistivity of the as-deposited PbS films was determined by the two point probe method. Fig. 11 shows the variation of resistivity of PbS thin films with temperature.

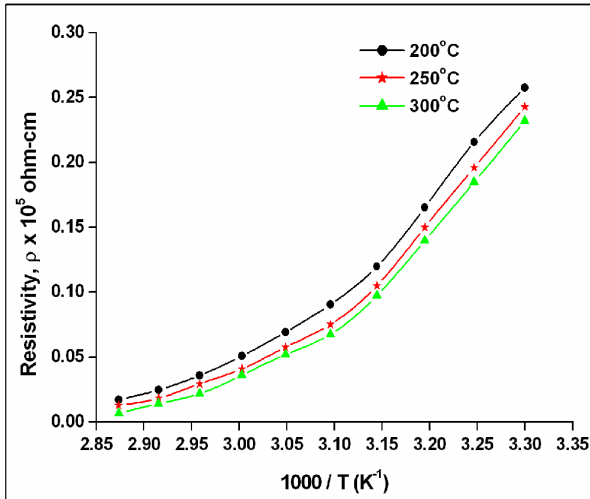


Fig. 11

#### Resistivity versus temperature graph of PbS films.

The resistivity value decreases with increase in temperature indicating the semiconducting nature of the films. The measured resistivity was found to vary in the range of  $0.105 \times 10^5$  ohm-cm to  $0.085 \times 10^5$  ohm-cm as the substrate temperature increases from 200 to 300°C. Generally the resistivity of PbS thin films depends on the factors: i) the removal of elemental sulfur and ii) chemisorption of oxygen in the PbS lattice. Removal of elemental sulfur from the PbS lattice takes place in a slow rate and the empty sites created in the got substituted by oxygen since the ionic radius of oxygen ( $-1.32 \text{ \AA}$ ) is lesser that of sulfur ( $-1.84 \text{ \AA}$ ). This might be the reason for the low value of resistivity obtained for the film coated at 300°C. Devika et al [45] obtained a high value of resistivity for spray pyrolysed SnS thin films grown at lower temperature ( $< 250^\circ\text{C}$ ) due to low grain size and high values of surface roughness. They also obtained a low value of resistivity for the film coated at temperatures  $> 275^\circ\text{C}$  due to free flow of carriers in the lattice due to larger grain size obtained. Similar argument can be applied here for the low resistivity value obtained for the PbS film coated at 300°C. The increased crystallite size obtained at 300°C (Table 3) strongly favors the above discussion for the reduced resistivity obtained.

M.Ozlas et. al [46] reported that improvement in crystallinity reduces the resistivity of sprayed ZnS thin films due to reduced grain boundary scattering. The high resistivity value for the PbS film coated at 200°C may be due to its poor crystallinity which indicates the presence of few atomic layers of disordered atoms [47]. Due to the disorderliness of atoms, large number of defects exists in the sample due to incomplete atomic bonding. This results in decreased carrier concentration as the traps became electrically charged after trapping the mobile carriers, creating a potential energy barrier which impeded the motion of carriers from one crystallite to another. The electrical conductivity and dislocation density are found to be directly related in all samples. The effect of substrate temperature on conductivity and dislocation density of PbS films is depicted in Fig. 12.

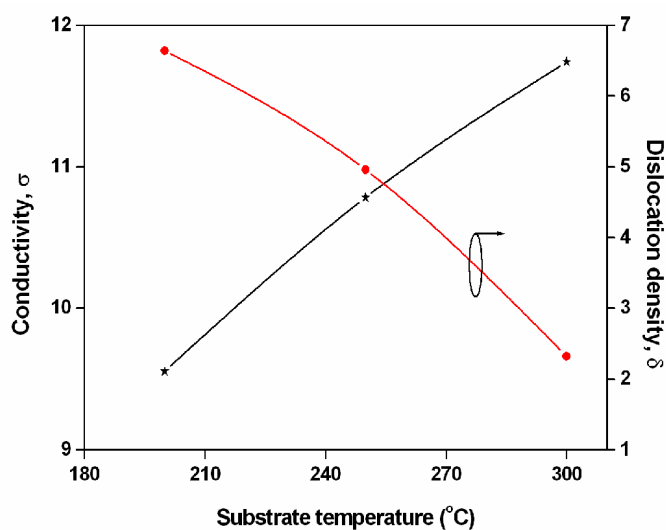


Fig. 12

Film coated at 300°C which is less strained having minimum dislocation density shows maximum electrical conductivity. Therefore, substrate temperature plays a vital role in the electrical conductivity of the PbS films in this study.

#### 4. Conclusions

PbS thin films were fabricated by spray pyrolysis technique on glass substrates at three different substrate temperatures. The effect of substrate temperature on the crystal structure, morphology, optical band gap and electrical properties of the as-deposited films has been investigated. XRD patterns suggested that the films were polycrystalline in nature with face centered cubic phase with a preferential orientation along the (1 1 1) plane. It was observed that the crystallinity increases with increase in substrate temperature. The SEM images showed that the film coated at 300°C is dense, smooth and uniform without pores. The low transmittance in the UV-Vis region and high reflectance in the IR region makes the films suitable for solar control coatings. Improved crystallinity makes  $E_g$  decreasing with increase in substrate temperature. The Urbach energy for the film coated at 300°C is low indicating a very weak absorption tail due to minimized defects and impurities. Refractive index value decreases from 2.8 to 2.35 as the substrate temperature increases from 200°C to 300°C. Packing density of PbS films coated at 300°C is high due to improved crystallinity. Electrical resistivity varies from  $0.105 \times 10^5$  ohm-cm to  $0.085 \times 10^5$  ohm-cm as temperature increases from 200°C to 300°C. Thus substrate temperature was one of the criteria that strongly influence film structure, crystallinity, optical properties and resistivity of spray deposited PbS thin films.

#### 5. Acknowledgements

The authors are grateful to the Secretary and Correspondent, AVVM Sri Pushpam College (Autonomous), Poondi for his excellent encouragement and support.

#### References

- [1] Colvin V.L., Schlamp, M.C. and Alivisatos, A.P., Light emitting diodes made from cadmium selenide, *Nature.*, 1994, 370, 354.
- [2] Klein D.L., Roth R., Lim A.K.L., Alivisatos A.P. and McEuen, P.L., Nanogap resistance random access memory based on natural aluminium oxide, *Nature.*, 1997, 389, 699.
- [3] Ridley B.A., Nivi B. and Jacobson J.M., All-Inorganic field effect transistors fabricated by printing, *Science.*, 1999, 286, 746.

- [4] Pentia E., Pintilie L., Matei I., Botila T. and Ozbaya E., Chemically prepared nanocrystalline PbS thin films, *J. Optoelectronics and Advanced Materials.*, 2001, 3( 2), 525.
- [5] Bass M., Vanstryland E.W., Williams D.R. and Wolfe W.L., *Handbook of Optics*, Vol. II, McGraw Hill, USA: 1995, pp,36.
- [6] Nair P.K., Nair M.T.S., Fernandez A. and Ocampo M., Properties of chemically deposited metal chalcogenide thin films for solar control applications, *J. Phys. D: Appl. Phys.*, 1989, 22, 829.
- [7] Venugopalan K., Thangavelu P.R., John S. and Rojendra S., Relationship between crystal morphology and photoluminescence in poly-nanocrystalline lead sulfide thin films, *Bull. Electrochem.*, 1994, 10, 504.
- [8] Nair P.K. and Nair M.T.S., PbS solar control coatings: safety, cost and optimization, *J.Phys, D: Appl. Phys.*, 1990, 23, 150.
- [9] Nair P.K., Ocampo M., Fernandez A. and Nair M.T.S., Spray pyrolytically deposited PbS thin films, *Sol. Energy.Mater.*, 1990, 20, 235.
- [10] Machol J.L., Wise F.W., Patel R.C. and Tanner D.B., Polarised photoluminescence from surface-passivated PbS nanocrystals, *Phys. Rev.*, 1993, B, 48, 2819.
- [11] Hirata H. and Higashiyama K., PbS crystals with clover like tructure, *Bull Chem. Soc. Jpn.*, 1971, 44, 2420.
- [12] Nair P.K., Gomezdaza O. and Nair M.T.S., Metal sulphide thin film photography with lead sulfide thin films, *Adv. Mater. Opt. Electron.*, 1992,1, 139.
- [13] Gadenne P., Yagil Y. and Deutscher G., Transmittance and reflectance in situ measurements of semiconductor gold films during deposition, *J. Appl. Phys.*, 1989, 66, 3019.
- [14] Chaudhuri T.K. and Chatterjee S., A solar thermophotovoltaic converter using PbS photovoltaic cells, *Int. J. Energy. Research.*,1992,16, 481.
- [15] Maheshwar Sharon., Ramaiah K.S., Mukul Kumar ., Neumann-Spallart M. and Levy C., Clement, Electrodeposition of lead sulfide in acidic medium, *Electroanal. Chem*, 1997, 436, 49.
- [16] Thangaraju B. and Kaliannan P., Spray pyrolytically deposited PbS thin films, *Semicond. Sci. Technol.*,2000, 15, 849.
- [17] Nair P.K., Garcia V.M., Hernandez A.B . and Nair M.T.S., Photoaccelerated chemical deposition of PbS thin films, *J. Phys. D: Appl. Phys.*, 1991, 24, 1466.
- [18] Yonghong Ni., Fei Wang., Hongjiang Liu., Gui Yin., Jianming Hong., Xiang Ma. and Zheng Xu., A novel aqueous phase route to prepare flower shaped PbS micron crystals, *J.Cryst. growth.*, 2004, 262, 399.
- [19] Yu Zhao., Xue-Hong Liao., Jian-Min Hong. and Jun-Jie Zhu., Synthesis of lead sulfide nanocrystals via microwave and sonochemical methods, *Mater. Chem. Phys.*, 2004, 87, 149.
- [20] Cristina Nascu., Valentina Vomir., Ileana Pop., Violeta Ionescu. and Rodica Grecu., The study of lead sulfide films : The behaviour at low temperature\_Thermal treatment., *Mater. Sci. Eng.*, 1996, B, 41, 235.
- [21] Larramendi E.M., Calzadilla O., Gonzalez – Arias, A., Hernandez E. and Ru Garcia J., Chemical solution deposition of semiconductor films, *Thin Solid Films.*, 2001, 389 , 301.
- [22] Pentia E., Pintilie L., Tivarus C., Pintilie I. and Botila T., Field effect assisted photoconductivity in PbS films deposited on silicon dioxide, *Mater. Sci. Eng.*, 2001, B 80, 23.
- [23] Rakesh K., Joshi., Alope Kanjilal. and Sehgal, H.K., Solution grown PbS nanoparticle Films, *Appl. Surf. Sci.*, 2004, 221, 43.
- [24] Valenzuela-Jauregui J.J., Ramirez-Bon R., Mondoza-Galvan A. and Sotelo- Lerma, M., Optical properties of PbS thin films chemically deposited at different temperatures, *Thin Solid Films.*, 2003, 441,104.
- [25] Ashour A., Afifi H. and Mahmoud S.A., Structural study of ZnS thin films prepared by spray pyrolysis, *Thin Solid Films.*, 1995, 263, 248.
- [26] Ashour A., Afifi H. and Mahmoud S.A., Structural, Optical and Electrical properties of CdS thin films obtained by spray pyrolysis, *Thin Solid Films.*, 1994, 248 , 253.
- [27] Nikale V.M., Gaikwad N.S., Rajpure K.Y. and Bhosale C.H., Structural and optical properties of spray deposited CdIn<sub>2</sub>Se<sub>4</sub> thin films, *Mater. Chem. Phys.*, 2002, 78, 363.
- [28] Rajpure K.Y. and Bhosale C.H., Preparation and characterization of spray deposited photoactive Sb<sub>2</sub>S<sub>3</sub> and Sb<sub>2</sub>Se<sub>3</sub> thin films prepared from aqueous and non-aqueous media.*Mater, Chem. Phys.*, 2002, 73, 6.
- [29] Afifi H.H., Aly, S.A., Abdal-Rahman, M. and Adbal – Hady, K. Electrochromic characterization of electrochemically deposited Nickel oxide films, *Physica B.*, 2000, 293, 125.

- [30] Shigesato, Y., Takaki S. and Haranoh T., Electrical and structural properties of low resistivity tin doped indium oxide films, *Appl. Surf. Technol.*, 1991,269,48 – 49.
- [31] Preetha K.C., Murali K.V., Ragina A.J., Deepa, K. and Ramadevi, T.L., Effect of cationic precursor pH on optical and transport properties of SILAR deposited nano crystalline PbS thin films, *Current Applied Physics.*, 2011,12, 53.
- [32] Ashour A., El-Kadry N., Ebid M.R., Farghal M. and Ramadan A.A., The electrical properties of CdTe films of different preparation conditions in correlation with microstructural changes, *Thin Solid Films.*, 1996, 279, 242.
- [33] Thangavel S., Ganesan S. & Saravanan K., Annealing effect on cadmium in situ doping of chemical bath deposited PbS thin films, *Thin Solid Films.*, 2012, 520 , 5206.
- [34] Tauc J., *Amorphous and Liquid Semiconductor*, Plenum Press, NewYork.,1974, 159.
- [35] Urbach F. The long wavelength edge of photographic sensitivity and electronic absorption of solids, *Phys., Rev.*, 1953, 92 ,1324.
- [36] Chopra K.L. and Das S.R., *Thin film solar cells*, Plenum Press, NewYork., 1983,256
- [37] Nair P.K. and Nair M.T.S., Preparation and characterization of chemically deposited PbS thin films, *J. Physics D: Applied Physics.*, 1990, 23, 150.
- [38] Subrahmanyam N.A., *A textbook of Optics*, 8<sup>th</sup> ed, Brj Laboratory, NewDelhi., 1977, 347.
- [39] Bendavid A., Martin P.J. and Wieczorek L., Morphology and optical properties of gold thin films prepared by filtered arc deposition, *Thin Solid Films.*, 1999, 354, 169.
- [40] Eya D.D.O. , Influence of thermal annealing on the structural and optical properties of PbO thin films prepared by chemical bath deposition technique, *Pacific.J.Sci and Technol.*, 2006,7 (2), 114.
- [41] Abbas M.M., Shehab A.Ab-M., Al-Samuraee A-K. and Hassan N-A., Effect of deposition time on the optical characteristics of chemically deposited nanostructured PbS thin films, *Energy Procedia.*, 2011, 6, 241.
- [42] Macleod H.A., Structure related optical properties of Thin films, *J. Vac. Sci. Technol.*, 1986, A. 4, 418.
- [43] Abdolazadeh Ziabari A. and Ghodsi F.E., Optoelectronic studies of sol-gel derived nanostructure CdO-ZnO composite films, *J.Alloys Compd.*, 2011, 509, 8748.
- [44] Wahab L.A. and Amer H.H., Composition dependence of optical constants of  $Ge_{1-x}Se_2Pb_x$  thin films. *Mater, Chem. Phys.*, 2006, 100, 430.
- [45] Devika M., Koteesware Reddy N., Ramesh K., Ganesan V., Gopal E.S.R. and Ramakrishna Reddy K.T., Influence of substrate temperature on surface structure and electrical resistivity of the evaporated tin sulphide films, *Appl. Sur. Sci.*, 2006, 253 ,1673 – 1676.
- [46] Oztas M., Bedir M., Neemeddin Yaziii A., Vural Kafadar E. and Toktamiz H., Characterisation of copper doped sprayed ZnS thin films. *Physica.*, 2006, B. 381, 40.
- [47] Seto J.Y.W., The electrical properties of polycrystalline silicon films, *J. Appl. Phys.*, 1976, 46 (12), 5247.

\*\*\*\*\*

CdTe is very suitable for thin film solar cells because it has direct band gap at room temperature. In the world PV market, the CdTe based solar cells have attained 16.5% efficiency. It has very good match with CdS on ITO glass substrate. The structural, chemical and physical properties depend on the deposition parameters and thickness of the thin film. The electrical, optical, and mechanical behavior of thin film also depends on microstructure, surface morphology, purity, and homogeneity. 3. Deposition techniques for thin films. The process by which thin film is deposited onto a substrate or onto a previously deposited layer is called thin film deposition. The process will be followed according to the requirements and economic conditions. The physical vapour deposition and its variants are often used because they offers many possibilities to modify the deposition parameters and to obtain film with determined structures and properties [25]. Depending upon preparation conditions, CdSe single crystals crystallizes either as sphalerite (cubic, zinc blende) structure with space group F 43m or as wurtzite (hexagonal, zinc selenide) structure with space group P3mc [26-28]. 2.2.2 Properties of Polycrystalline Thin Films. A solid material is said to be a thin film when it is built up as a thin layer on a solid support, called substrate. Composition of individual atomic, molecular or ionic species can be controlled during deposition either by physical processes and/or electrochemical reactions.